ELSEVIER

Journal of Structural Geology 27 (2005) 1282–1299

JOURNAL OF STRUCTURAL GEOLOGY

www.elsevier.com/locate/jsg

Opening and closing of folds in superposed deformations

Sudipta Sengupta[a,*], S.K. Ghosh[a], S.K. Deb[a,b], D. Khan[a,c]

[a]*Department of Geological Sciences, Jadavpur University, Kolkata 700 032, India*
[b]*Present address: Geological Survey of India, Kolkata 700016, India*
[c]*Present address: Department of Geology, Durgapur Govt. College, Durgapur, India*

Received 16 June 2003; received in revised form 25 May 2004; accepted 2 August 2004
Available online 6 July 2005

Abstract

During superposed deformation, an early fold (F_1) may either tighten or open out. Opening out is possible if, during the second deformation, there is a bulk extension across the F_1 axial plane. The theoretical model indicates that the rate of opening out is largely controlled by the initial tightness of the fold. The results of the numerical model are in agreement with analog experiments of superposed buckling and show that if there is a relatively small range of variation of initial tightness of F_1 folds, the range of fold tightness becomes much larger after the opening out of the folds in the second deformation. Consequently, the refolded structure may show a close association of different modes of superposed buckling. In a type-2 fold interference, the continued opening out of F_1 invariably causes a replacement of the initial F_1 hinge line by a new and more sinuous hinge line. When the shortening direction (P_2) of the second deformation was at an acute angle to the F_1-axis, depending upon their local orientation with respect to P_2, the F_1 folds were tightened in some places and were opened out elsewhere. When the enveloping surface is inclined in the direction of maximum stretching of second deformation, segments of F_1 and F_2 hinge lines may both rotate to lie in the extension field and both F_1 and F_2 may open out with progressive deformation. If F_1 has a low pitch, and P_2 is parallel to the F_1-axis, the two sets of hinge lines may become subparallel at an advanced stage of deformation. The resulting structure is morphologically similar to non-planar sheath folds.

Keywords: Superposed buckling; Opening folds; Hinge replacement; Modes of superposition

1. Introduction

The origin of different types of fold interference was first analyzed by Ramsay (1962, 1967, p. 518) in terms of the model of shear folding. These pioneering studies provided the first approximation to the complicated problem of the development of diverse morphological types of superposed folds. The majority of superposed folds in nature developed by superposition of buckling folds. Superposed buckling has been studied experimentally by a number of authors (e.g. Ghosh and Ramberg, 1968; Skjernaa, 1975; Watkinson, 1981; Odonne and Vialon, 1987; Ghosh et al., 1992, 1993, 1996; Grujic, 1993; Grujic et al., 2002; Johns and Mosher, 1996). The present study is essentially concerned with one aspect of superposed buckle folding that was not investigated in detail in previous theoretical or experimental studies.

The classic study of Flinn (1962) showed that superposed deformation might not always cause a tightening of the early folds during their refolding. Depending upon the orientation of the first fold axis and axial surface with respect to the principal axes of strain of the second deformation, the early folds may either open out or tighten, and may give rise to what has been described by Flinn (1962, p. 417) as *opening folds* and *closing folds*.

We shall first study the problem of opening out of the early folds by a theoretical analysis. This will be followed by experiments on superposed buckling in which there is a bulk extension in a flattening type of deformation.

2. Modes of superposed buckling and hinge replacement

The geometry of superposed buckling depends to a large extent on the initial tightness of early folds (Ghosh and Ramberg, 1968; Skjernaa, 1975; Watkinson, 1981; Odonne

* Corresponding author. Tel.: +91 33 412 7550; fax: +91 33 414 6375.
E-mail address: jugeossg@iacs.res.in (S. Sengupta).

0191-8141/$ - see front matter © 2005 Elsevier Ltd. All rights reserved.
doi:10.1016/j.jsg.2004.08.012

and Vialon, 1987; Ghosh et al., 1992, 1993, 1996; Grujic, 1993). In the experiments of superposed buckling by Ghosh and Ramberg (1968), two types were recognized. In one of these, small F_2 folds were superposed on larger F_1 folds. The F_2 folds rode over the hinges of larger open F_1 folds and gave rise to a type 1 interference pattern of Ramsay (1962). In the other type, the axial surfaces of close F_1 folds were folded to give rise to a type 2 interference pattern. These conclusions were confirmed by the experiments of Skjernaa (1975) and Watkinson (1981). In a further extension of this work, Ghosh et al. (1992) showed that, with increase in tightness of the initial folds, the superposed folds on a single embedded layer may show four different modes of buckling (Fig. 1). Two of these show type-1 interference and the other two show type-2 interference of Ramsay (1962). The dependence of the geometry of superposed buckling folds on the initial tightness of F_1 folds is much better explained if we consider all these four modes instead of describing the superposed folds in terms of only two types (types 1 and 2) of interference patterns.

If the early fold is very gentle and has a small curvature at the hinge zone, with a large interlimb angle (more than 135°), a dome-and-basin pattern or a type 1 interference pattern (Ramsay, 1967, p. 518; Ramsay and Huber, 1987, p. 492) is produced. This was described as mode 1 by Ghosh et al. (1992). The second mode of superposed buckling is produced when the first fold has a moderate tightness, with an interlimb angle of roughly 135–90°. In this mode, the F_2 folds are much smaller in size than the F_1 folds. The small F_2 folds ride over the hinges of large F_1 folds. This mode also belongs to the type 1 interference pattern of Ramsay (1967). The third mode of superposed buckling is produced when F_1 is initially fairly tight, with interlimb angle less than 90° but not very tight or isoclinal. The interference produces non-plane non-cylindrical folds; the curving of axial surfaces of the F_1 folds is associated with the process of *hinge replacement* (Ghosh et al., 1992, 1993, 1996). Occurrence of similar structures was also reported by Grujic (1993). The fourth mode of superposed folding also produces non-plane non-cylindrical folds but does not involve any hinge replacement. This mode of refolding is produced when the initial F_1 folds are very tight or isoclinal. The last two modes belong to type 2 interference (Ramsay, 1967, p. 518; Ramsay and Huber, 1987, p. 492). The geometry of the superposed buckling is greatly modified when the initial tightness of F_1 folds decreases due to opening out of the folds during second deformation.

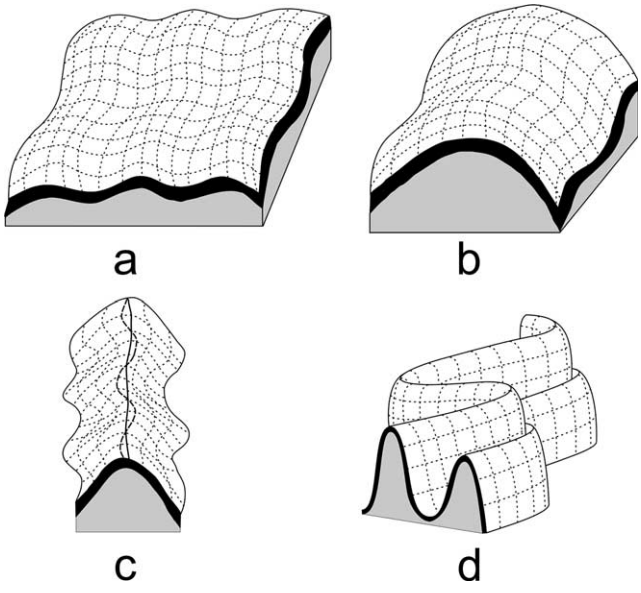

Fig. 1. Four modes of superposed buckling. (a) Mode 1, with domes-and-basin pattern. (b) Mode 2, where small F_2 fold ride over a large F_1 fold. (c) Mode 3, non-plane non-cylindrical folds with hinge replacement. (d) Mode 4, non-plane non-cylindrical folds without hinge replacement. After Ghosh et al. (1993).

The opening out of folds associated with a type 2 interference pattern is very often associated with the process of hinge replacement. During the development of non-plane non-cylindrical folds by buckling of plane cylindrical folds, the initial hinge lines of F_1 are replaced by a new hinge line F_1' (Fig. 2). This new hinge line is much more strongly curved than the deformed material line (Fig. 2a and b) that formed the initial hinge line. Hinge replacement associated with development of mode 3 of superposed buckling is quite distinct from the process of *hinge migration* described for the first time by Odonne and Vialon (1987, p. 839) in the context of superposed folding. In the experiments of Odonne and Vialon, hinge migration occurs when the angle between the two compressions, $Z1 \wedge Z2$ is low (30°,45°). The final product does not show two sets of folds. The early folds are transformed directly into cylindrical F_2 folds. Only *open* pre-existing folds are reused in this way. On the other hand during superposed buckling in the third mode, the early fold is *close*, not open, and the final structure is a non-plane non-cylindrical fold. The early fold hinge line is replaced by a curved F_1' hinge line at an angle to the F_2 hinge line. A characteristic feature of the process of hinge replacement (Ghosh et al., 1996) is that the arc-length of the curved new hinge line is larger than the length of the initial F_1 hinge line, even when the general trend of the new hinge line remains in the field of shortening of the second deformation (Fig. 2). This characteristic feature of hinge replacement is not shown by the process of hinge migration.

Earlier experiments on superposed buckling were mostly carried out by pure shear deformations under a situation in which there was no bulk extension across the axial surfaces of the first generation folds. The early folds, therefore, were tightened during later deformations. The morphology of the superposed folds is likely to be greatly modified when refolding of an early set of folds takes place concurrently with an opening out of folds.

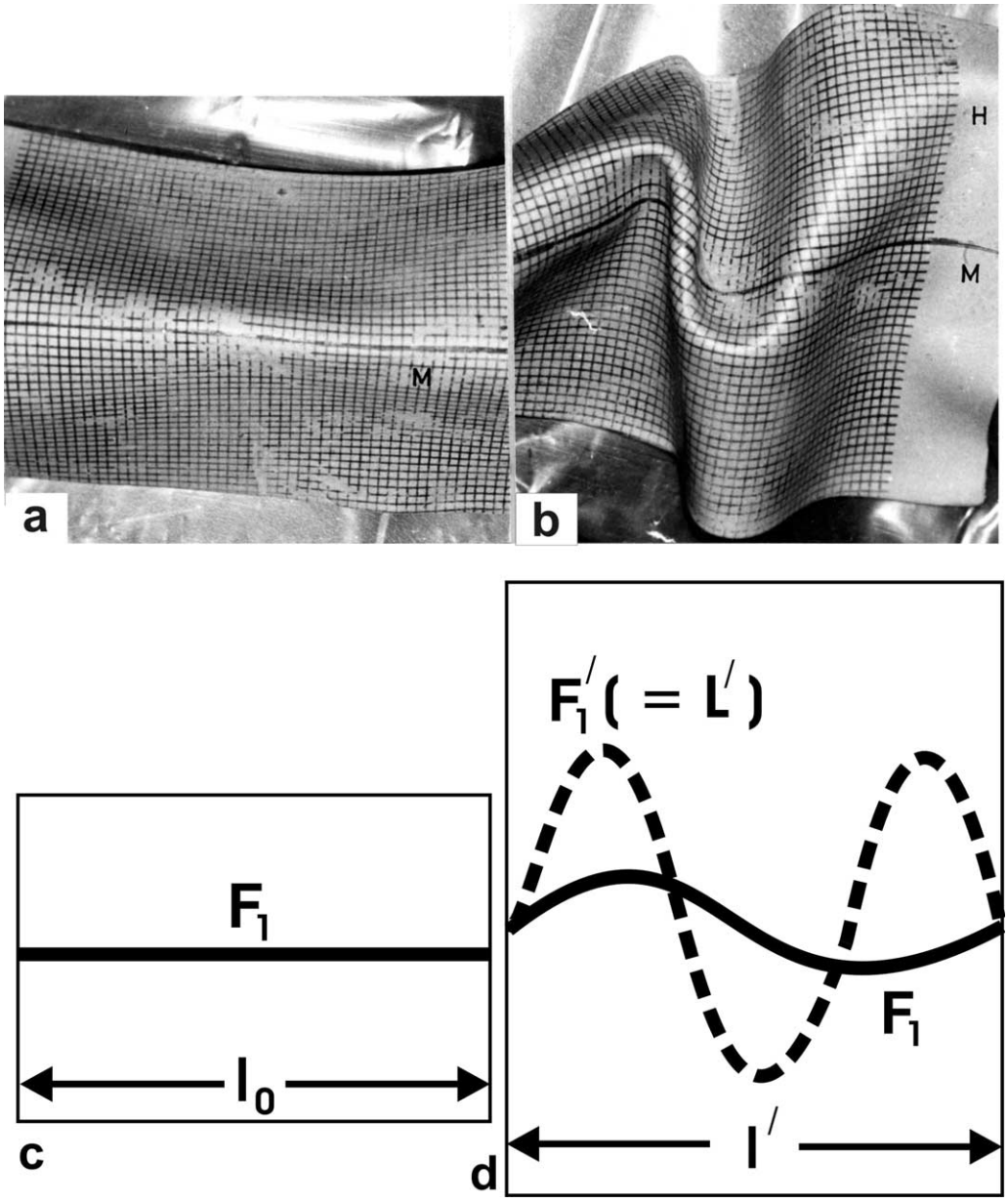

Fig. 2. Principle of hinge replacement shown with the help of a simple model. (a) Initial fold over a free sheet of modeling clay with grid lines. A black marker line (M) is drawn over the antiformal hinge F_1. (b) After the second deformation, the new hinge line H (F_1') is more sinuous than M (F_1). (c) Explanatory sketch to illustrate the process of hinge replacement. The early F_1 fold with initial length l_0. (d) After superposed buckling in mode 3, the new hinge F_1' is much more sinuous than the material line, which was parallel to F_1. The total shortening during the second deformation is $(l'-l_0)/l_0$. The arc-length L' is greater than l_0.

3. Numerical model of opening out of folds

3.1. General

The process of unfolding or opening out may take place by homogeneous deformation or by an external rotation of the limb segments of the fold. It is reasonable to assume that in nature the unfolding takes place by a combination of the two processes. An extremely competent layer can open out entirely by external rotation of limb segments. In most cases, however, there will be both an external rotation and homogenous strain. The homogeneous strain component causes not only a passive rotation of the limb segments but also an extension of the arc-length of the fold. In other words, the layer-length increases in course of the progressive deformation.

3.2. The initial fold

Let the middle surface of a sinusoidally folded layer be represented by the equation

$$y = a \sin nx, \tag{1}$$

where a and b are the amplitude and quarter wavelength

(Fig. 3a), with

$$n = \frac{2\pi}{4b} = \frac{\pi}{2b}. \tag{2}$$

The tightness of this initial fold is measured either by the ratio (a/b) or by the interlimb angle (IA). The dip angle (θ) is obtained from the equation

$$\tan\theta = \frac{dy}{dx} = an\cos nx. \tag{3}$$

At the point of inflection $x=0$

$$\tan\theta_0 = an. \tag{4}$$

The interlimb angle (IA) (Fig. 3b)

$$\mathrm{IA} = 180^\circ - 2\theta_0. \tag{5}$$

The length of arc of this initial fold is

$$s = \int_0^x \sqrt{1 + (dy/dx)^2}\,dx. \tag{6}$$

With $nx=z$, where n is given by Eq. (2), Eq. (6) can be written, with some simplification, as

$$s = \frac{\sqrt{1+a^2n^2}}{n}\int_0^z \sqrt{1 - k^2\sin^2 z}\,dz, \tag{7}$$

where

$$k^2 = \frac{a^2n^2}{1+a^2n^2}, \tag{8}$$

or

$$s = \frac{\sqrt{1+a^2n^2}}{n}E(k,z), \tag{9}$$

$E(k,z)$ being the elliptic integral of the second kind (Hancock, 1958; Ghosh and Chatterjee, 1985). The length of arc over a quarter wave is

$$L = \frac{\sqrt{1+a^2n^2}}{n}E, \tag{10}$$

where E is the complete elliptic integral of the of the second kind. From Eq. (8), it is found that

$$\sqrt{1+a^2n^2} = \frac{1}{\sqrt{1-k^2}}. \tag{11}$$

Hence, Eq. (10) can be written as

$$L = \frac{E}{n\sqrt{1-k^2}}. \tag{12}$$

E can be determined either from a table of complete elliptic integrals (Belyakov et al., 1965) or from the infinite series

$$E = \int_0^{\pi/2}\sqrt{1-k^2\sin^2 z}\,dz$$

$$= \frac{\pi}{2}\left[1 - \left(\frac{1}{2}\right)^2 k^2 - \left(\frac{1.3}{2.4}\right)^2\frac{k^4}{3} - \left(\frac{1.3.5}{2.4.6}\right)^2\frac{k^6}{5} - \left(\frac{1.3.5.7}{2.4.6.8}\right)^2\frac{k^8}{7}\cdots\right]. \tag{13}$$

3.3. Opening out by homogeneous strain and external rotation

Let the rate of natural strain along the x-direction be $\dot{\varepsilon}_x$, and let the ratio of the rates of extension by homogeneous strain ($\dot{\varepsilon}_h$) and external rotation ($\dot{\varepsilon}_r$) be a constant A

$$A = \frac{\dot{\varepsilon}_r}{\dot{\varepsilon}_h}. \tag{14}$$

For a small increment $\Delta\varepsilon_x$

$$\Delta\varepsilon_r = \Delta\varepsilon_h A, \tag{15}$$

$$\Delta\varepsilon_x = \Delta\varepsilon_h + \Delta\varepsilon_r \tag{16}$$

so that

$$\Delta\varepsilon_h = \frac{\Delta\varepsilon_x}{A+1}, \tag{17}$$

$$\Delta\varepsilon_r = \frac{A}{A+1}\Delta\varepsilon_x. \tag{18}$$

The opening out of the fold by simultaneous homogeneous strain and external rotation is approximated by

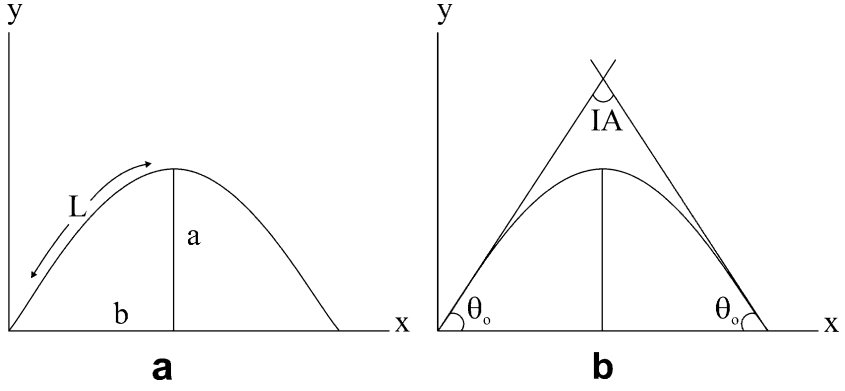

Fig. 3. (a) A sine curve with amplitude a, quarter wavelength b. L is length of arc over the quarter wave. (b) The interlimb angle (IA) of the folded layer is $(180^\circ - 2\theta_0)$.

taking a succession of small steps of homogenous strain and external rotation.

Step 1: *Increment of homogeneous strain*

If the initial length of the quarter wave is b, its value after an increment of $\Delta\varepsilon_h$ is b_h

$$b_h = b \exp\left(\frac{1}{A+1}\Delta\varepsilon_x\right). \tag{19}$$

The amplitude (a) remains unchanged during this increment. The arc-length is changed by this incremental homogeneous strain

$$L_h = \frac{\sqrt{1+a^2n_h^2}}{n_h}E \tag{20}$$

where $n_h = \pi/2b_h$ and E is the complete elliptic integral corresponding with the current value of k

$$k_h^2 = \frac{a^2n_h^2}{1+a^2n_h^2}. \tag{21}$$

Step 2: *Increment of external rotation*

Let the next incremental extension along the x direction be b_r

$$b_r = b_h \exp\left(\frac{A}{A+1}\Delta\varepsilon_x\right). \tag{22}$$

Since this change in the quarter wavelength takes place by external rotation alone, the length of arc of the fold remains unchanged in this step. It should be noted that after the increment of homogeneous strain the fold shape remains a sine wave $y' = a \sin nx'$. We have assumed that the fold shape remains a sine curve even after incremental external rotation. As the quarter wavelength has changed to b_r and the length of arc has remained unchanged at L_h, the problem is to find the fold amplitude (a) while the fold profile remains a sine curve. The length of arc is

$$L_r = L_h = \frac{E}{n_r\sqrt{1-k_r^2}}, \tag{23}$$

where $n_r = \pi/2b_r$. In the computations, the previous value of k (i.e. that value of k in the earlier step) was reduced repeatedly by a small amount (0.0001), E was determined by taking a large number (20) of terms of Eq. (13) and L was calculated from Eq. (23). The computation was repeated by taking successively lower values of k^2 till $|(L_r - L_i| \leq 0.0001$. The amplitude was determined from the final value k_r

$$a_r = \frac{k_r}{n_r\sqrt{1-k_r^2}}. \tag{24}$$

The interlimb angle of the fold at this step is obtained from Eqs. (4) and (5).

Steps 1 and 2 constitute one cycle of computation of homogeneous strain and external rotations. In the next cycle of computation, the amplitude, quarter wavelength and length of arc obtained in step 2 are taken as initial values of step 1.

In the numerical examples, we have considered five folds (Fig. 4) with different initial tightness:

(1) $a=1$, $b=1$, $\theta_0=57.5°$, IA$=65°$
(2) $a=1.5$, $b=1$, $\theta_0=67°$, IA$=46°$
(3) $a=2$, $b=1$, $\theta_0=72.3°$, IA$=35°$
(4) $a=3$, $b=1$, $\theta_0=78°$, IA$=24°$
(5) $a=5$, $b=1$, $\theta_0=82.7°$, IA$=14.5°$

For each of these folds, we have taken three values of A, i.e. $A=10$, 5 and 2.

3.4. Numerical results of the model of opening out of folds

The results of the numerical calculations from the theoretical model are presented in Figs. 4 and 5. The results indicate that the rate of decrease in tightness or rate of increase in the interlimb angle (IA) of a fold, with respect to the rate of bulk strain, is mainly dependent on the initial IA of the fold. A small difference in the initial IA may cause a large difference in the rate of opening out of the fold. Fig. 4b shows the change in interlimb angle with progressive deformation for folds with five different initial IA. The folds range from very tight (IA$=14.5°$) to moderately close (IA$=$ $65°$). For each fold, the rate of change in IA increases with progressive deformation. Again, for each stage of deformation, the rate of change of IA increases with increasing values of interlimb angle. In other words, a very tight fold opens out at a much smaller rate than a close fold. As a consequence, if we have a set of initial folds with a certain range of tightness, the opened out folds of the set at any stage of deformation have a much larger range of tightness. With progressive deformation, this range of tightness rapidly increases. As an example, let us consider five folds with initial tightness ranging from 14.5 to 65°. At a stage of deformation with $\varepsilon_x=0.2$, this range increases from 15 to 90°. Again at $\varepsilon_x=0.4$, this range is from 21 to 132° (Fig. 4).

As mentioned earlier, the mode of buckling depends upon the initial IA. The model considered by us shows that, even if there is a small range of variation of initial tightness, the superposed buckling may cause interfering folds in quite different modes.

The ratio (A) of rate of external rotation to layer-parallel homogeneous strain is a measure of the competence contrast between the layer and its embedding medium. This ratio does not significantly alter the rate of opening out of the folds up to moderate values of deformation (curve 4 in Fig. 4). It does, however, determine the change in the arc-length of the fold with progressive deformation. The ratio of change in arc-length remains very small when the fold is very tight (Fig. 5c); it increases with decreasing tightness of the initial folds (Fig. 5a and b). Fig. 5a and b shows the change of arc-length for folds with initial interlimb angles of

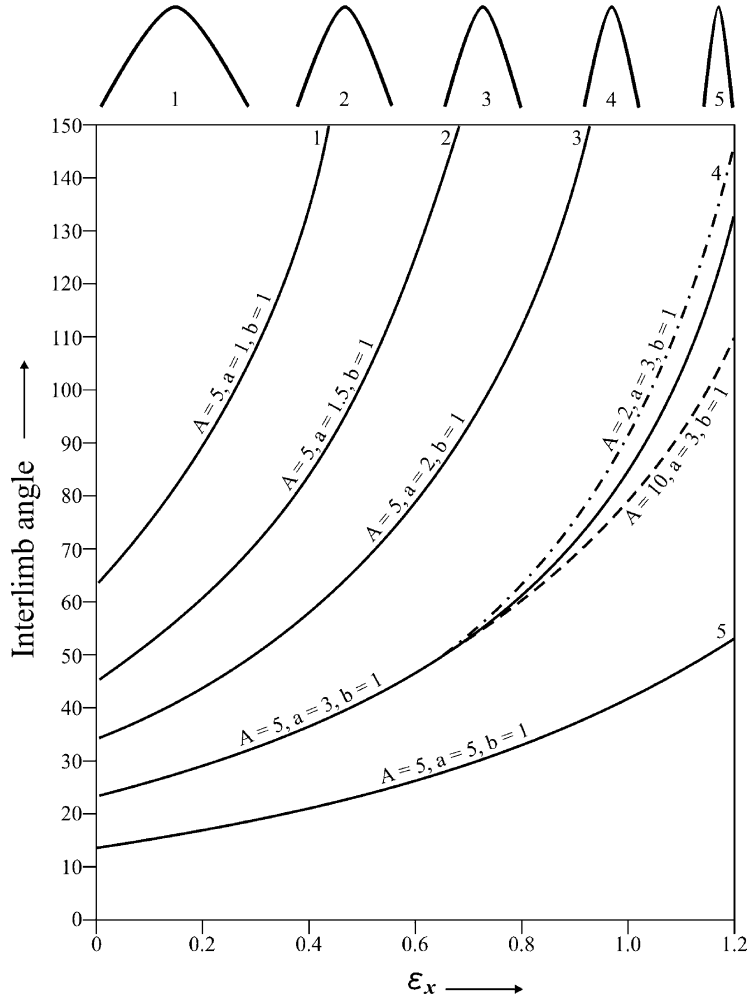

Fig. 4. Five folds with interlimb angles of 65, 46, 35, 24, and 14.5° (top). Curves showing changes in interlimb angles (IA) with progressive deformation (ε_x) at $A=5$. A is the ratio between the rate of extension by homogeneous strain and external rotation, a and b as shown in Fig. 3. Curves 4 (with interlimb angle 24°) shows variations at $A=2$ and 10. The rate of change of IA increases with increase in initial tightness. For each case, the rate of opening out increases with progressive deformation.

35 and 24°, respectively. For the folds, the arc-length increases rapidly for small values of A. Hence, the folds open out faster for more competent layers. The rate of change in arc-length in any type of fold increases with progressive deformation.

In the history of progressive tightening of buckling folds, it is generally assumed that the rate of tightening by external rotation is a maximum when the interlimb angle is 90°. This rate tends to vanish when the interlimb angle is 180 or 0°. The opening out of the folds may also depend on the initial shape. However, it is unlikely that it will be similar to that of progressive tightening. Thus, for example, for a tight or isoclinal fold, it is assumed that the limbs became 'locked'. No such 'locking' is required for the opening out of the isoclinal or very tight folds. During progressive tightening, no further change in the interlimb angle of an isoclinal fold is possible. An isoclinal fold may, however, show an appreciable rate of opening out. It is likely that the process of opening out by external rotation is more complex. This problem has not been considered in our model.

4. Opening and closing folds in experiments of superposed buckling: experimental method

The experiments were carried out with models of 2-mm-thick single layer of modeling clay embedded in painters' putty. The model materials are the same as in our previous experiments on superposed buckling (Ghosh et al., 1992, 1993, 1995, 1996). Modeling clay and painter's putty were used for competent layers and the matrix, respectively. In most of the experiments, the model was first deformed by pure shear to produce the F_1 folds. In a few experiments, the F_1 folds were artificially induced as in Ghosh et al. (1992, p. 382). In both cases, a slice of the model was cut perpendicular to the fold axis from two opposite sides of the model to reveal the geometry of the initial F_1 fold. The

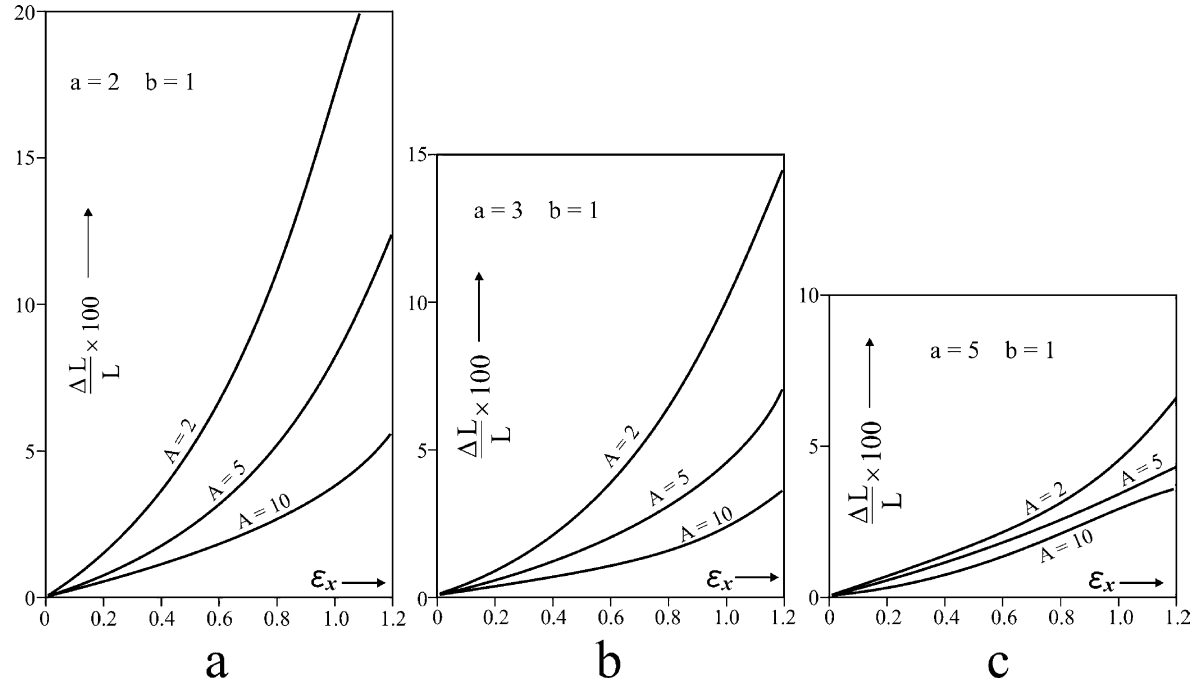

Fig. 5. Curves showing relationship between extension of arc-length and deformation (ε_x) of three folded layers with different values of interlimb angles. (a), (b), and (c) refer to initial folds with interlimb angles 35, 24, and 14.5°, respectively. A is the ratio of the rates of extension by homogeneous strain and external rotation. With progressive deformation, the arc-length increases at a faster rate for less tight folds ((a) and (b)) and for more competent layers at small values of A.

interlimb angle of F_1 was measured from these sections. The second deformation was by uniaxial compression where the model could extend in two directions perpendicular to the direction of compression. After the second deformation, the overburden of putty was removed to expose the fold interference pattern on the competent layer of modeling clay.

A problem for these experiments is to find a method of measuring tightness of the folds after the second deformation without destroying the model itself. Some idea about the magnitude of opening out can, however, be obtained from the following considerations. As mentioned above, the tightness of the initial F_1 folds can be obtained from the sections of the model cut from the opposite edges perpendicular to the F_1-axis. The number of waves (N) of F_1 does not change in the course of opening out. The average wavelength (W), however, increases because of opening of folds:

Average wavelength

= Width of model (L) perpendicular to F_1/Number of waves (N)

: $W = L/N$.

Since N remains the same in the course of deformation, a measure of tightening or opening out can be obtained from the average value of W after the second deformation. This kind of comparison should be made from each model before and after deformation. Thus, for the model shown in Fig. 9, the initial value of W was 1.3 cm. After the second deformation, the average wavelength became 2.1 cm. This method is approximate because it does not take into consideration the extension of the layer by homogeneous strain. On the other hand, it has the advantage that the measurement can be made without cutting up the model to reveal the transverse sections.

To describe the geometry of the structures, a co-ordinate system is chosen with y- and z-axes horizontal and x-axis vertical. The direction of maximum shortening P_2 coincides with the horizontal z-axis. The experiments were classified into five categories. In each case, the maximum bulk shortening remained horizontal. The geometry of the F_1 fold with respect to P_2 varied in different models (Fig. 6):

1. Horizontal enveloping surface with horizontal F_1-axis. The deformation was by uniaxial compression. The direction of compression P_2 was parallel to the F_1-axis (Fig. 6a). The model was free to extend in a vertical direction as well as in the horizontal direction perpendicular to the F_1 axial planes.
2. The enveloping surface was horizontal but the F_1-axis was oblique ($<30°$) to the direction of maximum compression P_2 (Fig. 6b).
3. The enveloping surface was inclined and the F_1-axis on it had a large pitch; P_2 was along the dip direction of the enveloping surface. The deformation was by uniaxial compression (Fig. 6c).
4. The enveloping surface was inclined but P_2 was parallel

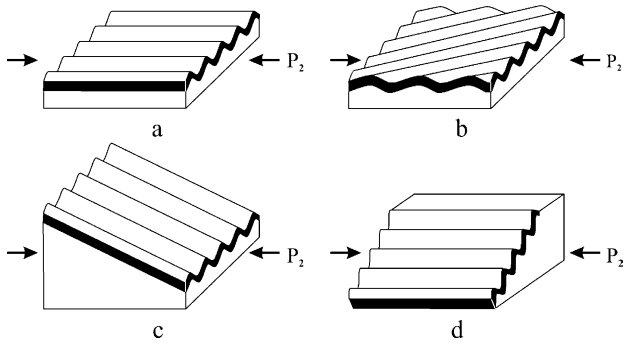

Fig. 6. Orientation of F_1-axes and the enveloping surfaces of the folded layer at different experiments of superposed buckling. P_2 shows the direction of compression during second deformation.

to the horizontal F_1-axis (Fig. 6d). The deformation was by pure shear. There was an extension along the vertical direction (x-co-ordinate axis) and no bulk strain along the y-co-ordinate axis.

5. Similar to the first set of experiments (Fig. 6a) but instead of a single layer, a pack of multilayer was used with the number of individual layers within it varying between 8 and 12.

There is some heterogeneity in some of the models. The heterogeneity, the variation in the tightness of the folds results from friction at the vertical sidewalls that compress the model horizontally. There is also friction between the model and the base on which it rests. The friction cannot be avoided altogether but can be reduced substantially by applying liquid soap or oil as lubricants. Floating the model on mercury (Ghosh and Ramberg, 1968) practically eliminates the friction at the base, but recovering the mercury from the base of the deformed model is a messy process and involves health hazard. On the whole, if the base and the sidewalls are well lubricated, a fairly large (compared to the wavelength of the folds) domain in the central part of the model can be obtained in which the strain is essentially homogeneous, i.e. the wavelengths of F_1 and F_2 are fairly regular.

5. Experimental results

5.1. Superposed buckling in horizontal layer with P_2 parallel to F_1 fold axes

Eight experiments were performed in this series. In five of these, F_1 was produced by layer-parallel shortening in pure shear deformation. In three models, a series of folds was artificially induced. Most of the F_1 folds of these models were moderately tight to very tight folds. Some of the folds were isoclinal.

As mentioned above, there is some inhomogeneity of the opening out of the F_1. Thus, for example, in the model shown in Fig. 7, the nearly isoclinal initial F_1 folds opened out in most domains. However, at the right hand edge of the model (Fig. 7a and b), the opening out was inhibited. As a result, the F_1/F_2 interference in this domain was in mode 4 of Ghosh et al. (1992). In other words, the F_1 folds were deformed to produce non-plane non-cylindrical folds without hinge replacement. Elsewhere, where the F_1 folds opened out, the opening out of F_1 was associated with hinge replacement in mode 3 of superposed buckling (Fig. 7c), giving rise to a characteristic triangular shape of the folds (Ghosh and Ramberg, 1968, fig. 9; Ghosh et al., 1992, fig. 5).

The hinge replacement associated with development of the third mode of superposed buckling of an opened out tight fold can be very clearly seen in the model shown in Fig. 8. The development of triangular folds is also very clearly seen in Fig. 8b. It should be noted that during the second deformation the opening out of F_1 and the superposition of F_2 took place concurrently and the opening out may continue with F_2 folding even after formation of the mode 3 superposed folds. This gave rise to a greatly opened out F_1 (with moderate to low tightness) but still retaining the non-plane non-cylindrical geometry of mode 3 superposed folds (Figs. 7 and 8c). All earlier experiments (Ghosh and Ramberg, 1968; Skjernaa, 1975; Watkinson, 1981; Ghosh et al., 1992, 1993, 1996; Grujic, 1993) show that non-plane non-cylindrical folds cannot develop unless the folds are at least moderately tight. Hence the structure described above can only develop if superposed folding is associated with concurrent opening out of F_1.

In models shown in Figs. 7 and 8, where the initial folds were very tight or isoclinal, the concurrent opening out of folds produced non-plane non-cylindrical folds of the third mode. When the initial folds are moderately tight, the concurrent opening out produced a structure showing superposed folds of second mode. In these models, the initial F_1 folds have opened out to open folds with interlimb angles varying between 135 and 90°. Consequently, small F_2 folds ride over larger F_1 folds in mode 2 (Fig. 9). This would not have been possible if the initial tight folds had not opened out. The opening out F_1 folds continued even after development of second mode of superposed buckling. With continued deformation, a set of tight small F_2 folds was seen to ride over gentle large F_1 folds. The association of gentle F_1 with small tight F_2 in the current experiments is essential because of the opening out of F_1 during superposed deformations.

Fig. 10 shows a model with initial F_1 folds having a larger interlimb angle (around 60°). There was a significant opening out of the F_1 folds in the central part and the superposed buckling is in mode 1, with a dome-and-basin pattern. With progressive deformation, we get tighter F_2 folds and very gentle F_1 folds. Towards the edges of the model, F_1 folds remained tighter and the superposed folds were in second mode.

The opening out of a buckling fold takes place partly by external rotation and partly by homogeneous strain. The

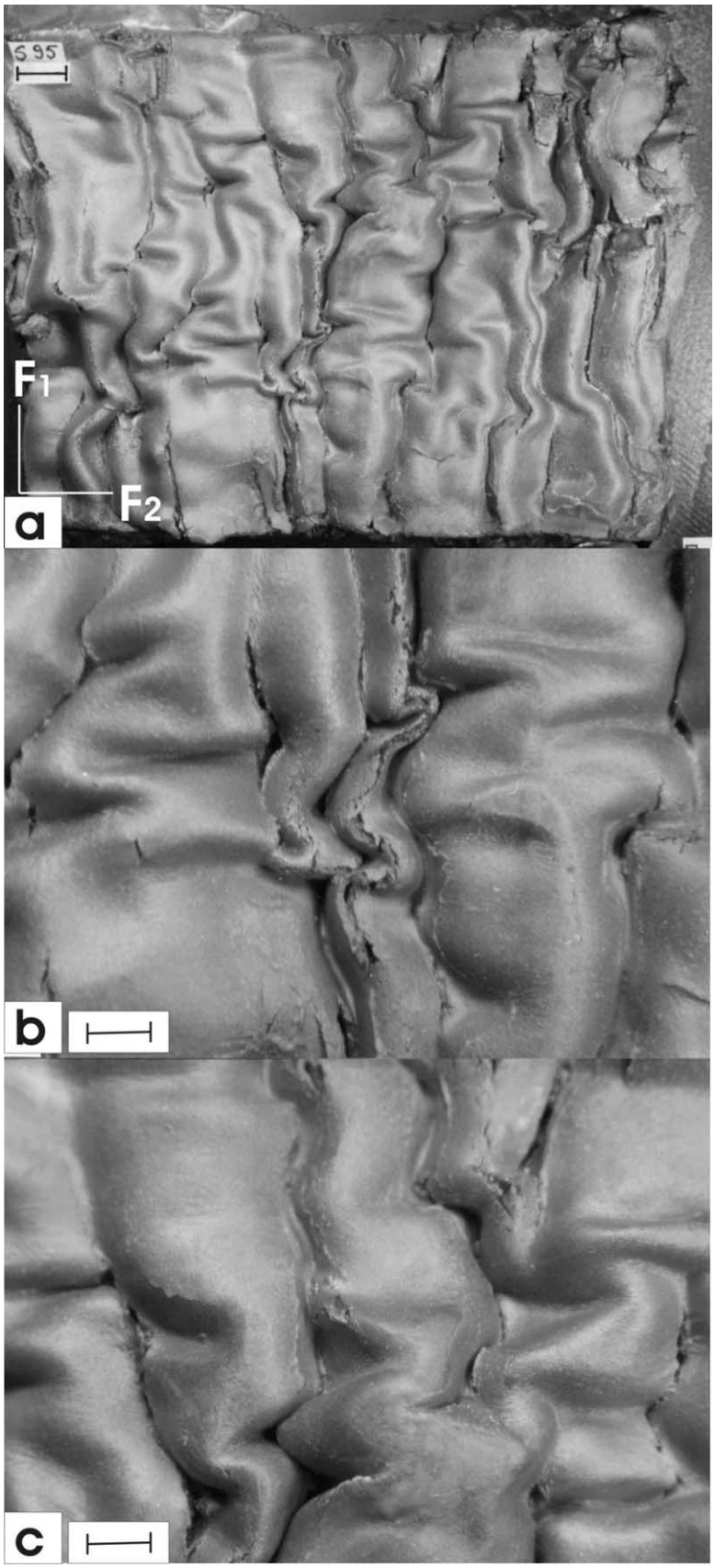

Fig. 7. (a) Superposed buckling with interference of F_1 and F_2 after removal of the overburden of putty. Scale bar is 1 cm. (b) Details of the model with fourth mode of superposed folding of an isoclinal F_1 fold. (c) Details of the model showing the typical triangular shape of third mode of superposed buckling with hinge replacement. Scale bar in (b) and (c) is 0.5 cm.

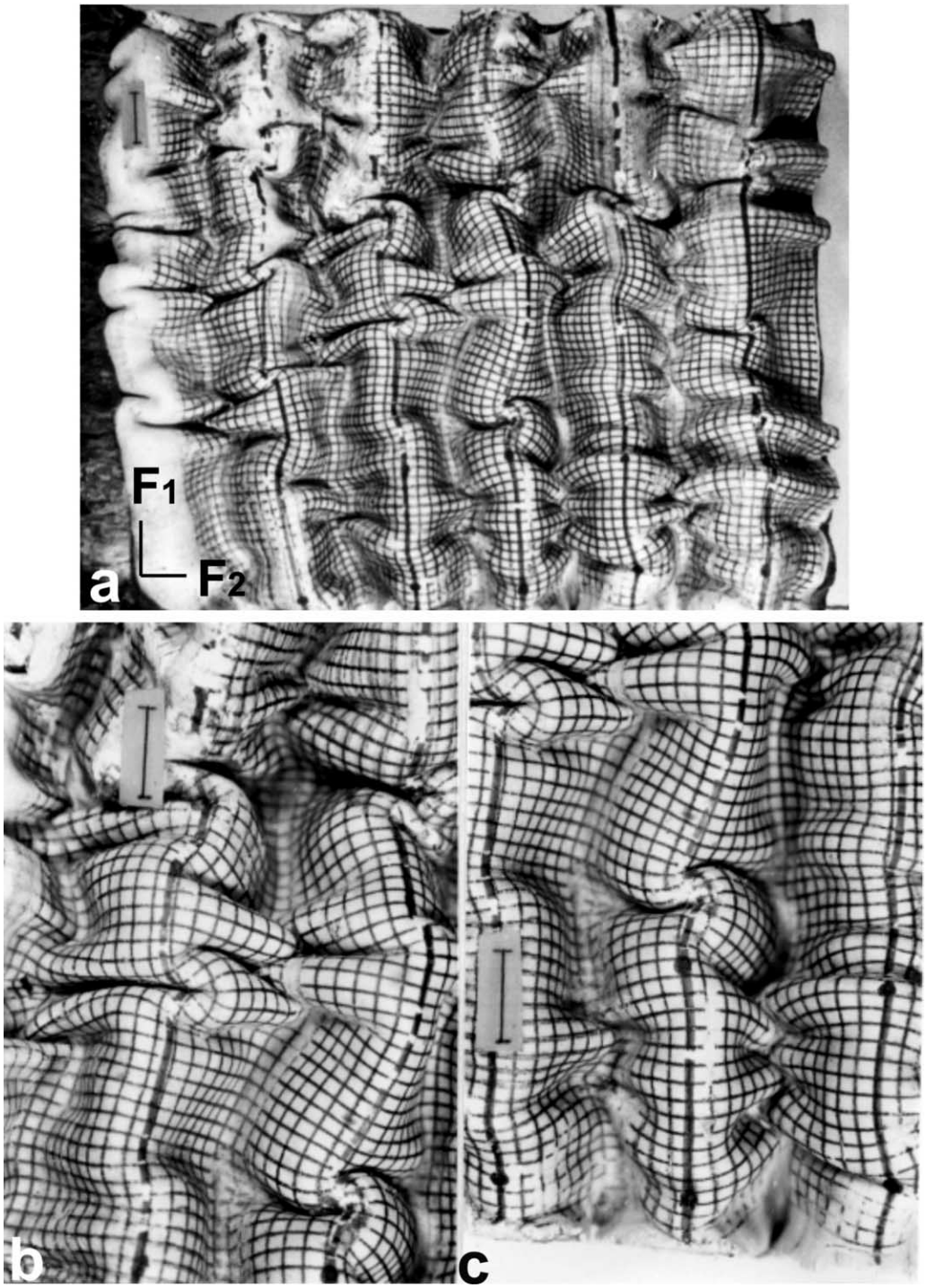

Fig. 8. Opening out of F_1 folds during second deformation showing superposed folds in the third mode in most places. (b) and (c) Details of the model. The early F_1 hinges (marked by bold black lines) are replaced by more sinuous new hinge during second deformation. F_2 folds show triangular shapes of third mode. Scale bar is 1 cm.

total extension of the layer across the F_1 axial surface in the y-direction did not take place entirely by an opening out of F_1 folds by external rotation; a considerable part of it was by layer-parallel homogeneous strain. This is illustrated in Fig. 11a. The initial length of the layer in the model was 21 cm. After the development of the first set of folds, the length of the model across the F_1 axial surface was 15 cm. After the second deformation, the length of the model along the same direction became 22 cm, i.e. greater than the initial length. If the F_1 folds were unrolled completely by external rotation

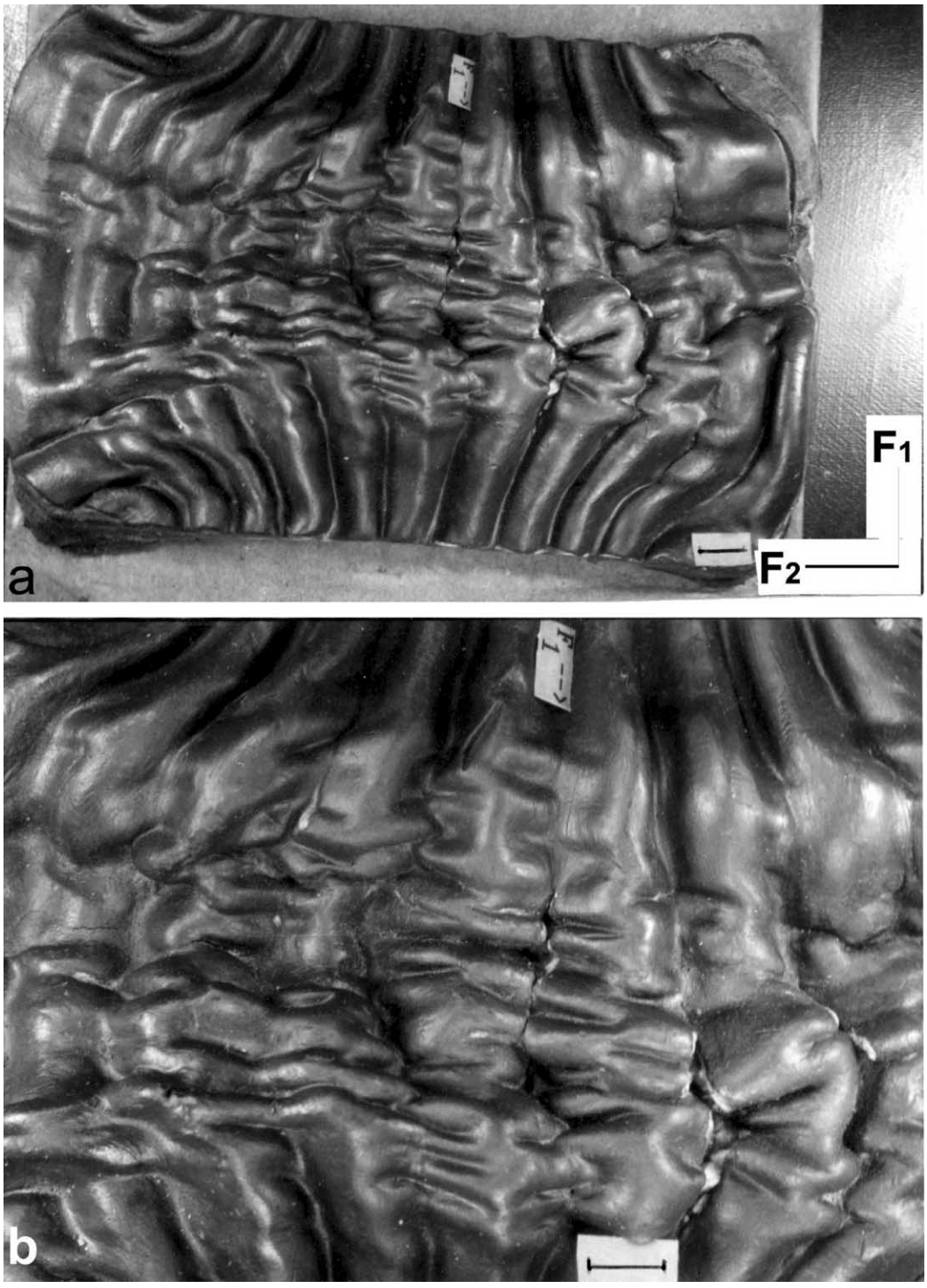

Fig. 9. (a) Superposed buckling associated with opening out of early folds after removal of the overburden. F_1 folds have opened out more at the central part. (b) Details of the central part of the model shown in (a). Superposed buckling in mode 2 with tight F_2 folds over gentle F_1 folds. Scale bar is 1 cm.

alone, the extension would have been 40%. However, the extension now is 46.7%. Since the layer still shows some significant undulation around F_1-axis, the extension by layer-parallel homogeneous strain must be more than 6.7%. The maximum extension along the x-direction took place along the central segment of the model.

5.2. Superposed folding in horizontal layers with P_2 oblique F_1-axis

After the first deformation to produce a set of F_1 folds, the model was then cut into a smaller rectangular block in such a manner that, when placed in the apparatus of uniaxial

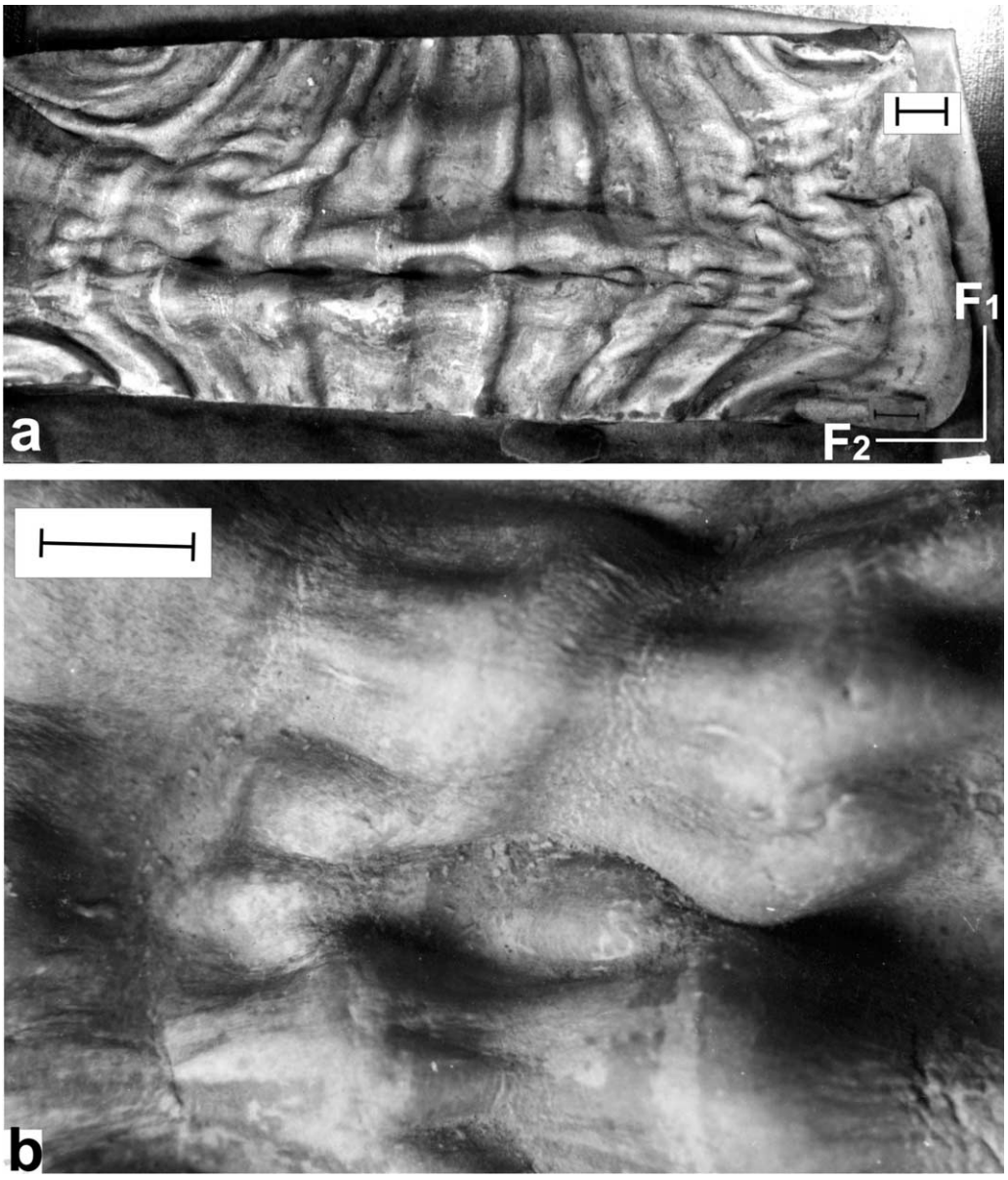

Fig. 10. (a) Opening out of the F_1 folds to a great extent during refolding produced dome-and-basin patterns. At the edges of the model, the F_1 folds did not open out to the same extent as in the central part, and the superposed buckling is in the second mode. (b) Details of the model shown in (a). Scale bar is 1 cm.

compression, the direction of bulk shortening was at an angle to the F_1-axis (Fig. 6b). The model was free to extend in the vertical y-direction and horizontal x-direction perpendicular to P_2. The angle between P_2 and the F_1 fold axes was 10, 15 and 20° in different models.

In the model in which the angle between P_2 and F_1 was 10°, the morphology of the superposed folds was more or less similar to the previous case. In the other models, there was a significant amount of rotation of F_1 fold axes and axial surfaces away from the direction of shortening. With progressive shortening during the second deformation, the F_1-axes were affected by an overall rotation of hinge lines towards the stretching direction (passive reorientation of F_1-axes) and variable rotation due to superposed buckling resulting in asymmetric folding of hinge lines and axial surfaces (active reorientation of F_1-axes). In addition, there was a development of a new strongly curved hinge line due to hinge replacement in the third mode of superposed buckling.

Where the reorientation of the F_1 hinge line was mainly achieved by development of non-plane non-cylindrical folds, with an asymmetric curving of the F_1 hinge lines, the different segments of the hinge lines were at different angles with P_2. Depending upon the local orientation of the hinge line and axial surfaces with respect to P_2, the folds were in some places in the extension field and elsewhere in the compression field. Where the F_1 hinge lines were rotated to assume low angle to P_2, the fold opened out. On the other hand, where a segment of F_1 hinge was at a high angle to P_2 ($>45°$), there was tightening of the F_1 fold. Hence across

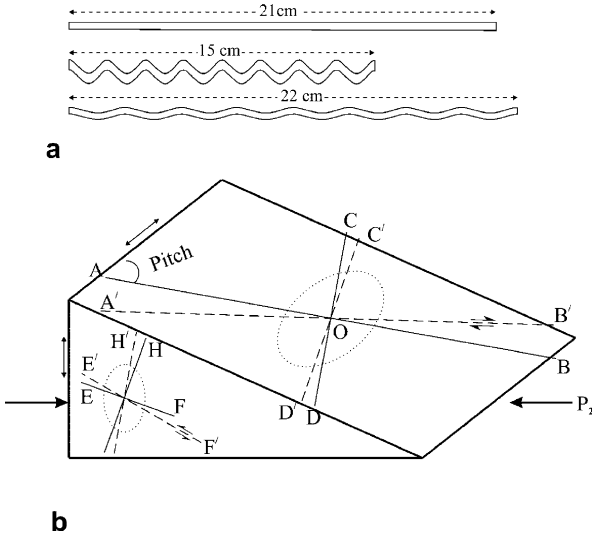

Fig. 11. (a) Diagrammatic sketch of opening out of folds partly by external rotation and partly by layer-parallel strain. (b). Sense of shear on an inclined plane with F_1 at an angle to P_2. The bulk strain is of flattening type. Sectional strain ellipses are shown on the inclined surface and on the vertical face. AB is the orientation of the fold axis on the enveloping surface at a certain stage of deformation. CD is a line normal to AB and lying on the inclined enveloping surface. With progressive deformation, AB and CD have rotated to the positions A′B′ and C′D′, so that both these lines come closer to the long axis of the strain ellipse which at an early stage of deformation is parallel to the strike of the enveloping surface. The sense of shear can be obtained from the reduction in the right angle between the two sets of line. Similarly on a vertical face of the model at a right angle to the strike of the enveloping surface, EF is a line parallel to the dip direction and GH is at right angle to it. Since on this vertical face parallel to the *XZ* plane of strain ellipse, *X* is vertical, both EF and GH will rotate towards the vertical direction. The sense of shear will be upper part up-dip.

Fig. 12. Superposed buckling with horizontal sheet with $F_1 \wedge P_2 = 20°$. Due to local variation of orientation with respect to P_2, the F_1 fold is opened out in some domains and tightened in the other domains (central part). Scale bar is 1 cm.

the sinuous axial surface of the buckled F_1 fold, there was a tightening in some places and opening elsewhere (Fig. 12). Where the opening fold had assumed a moderate tightness, and the hinge line at the same time was at a large angle with P_2, the F_1 hinge line was replaced by a strongly curved new hinge line by superposed buckling in the third mode (lower part of model S49 in Fig. 12).

5.3. Superposed buckling of inclined enveloping surfaces with a large pitch of F_1-axis

Experiments on superposed buckling on inclined enveloping surfaces were carried out with two sets of models. The dip of the enveloping surfaces varied from 15 to 20°. In one of these sets, the pitch of F_1 ranged between 65 and 90°. The shortening direction of the second deformation was horizontal and parallel to the dip direction of the enveloping surface (Fig. 6c).

For a 90° pitch of F_1, the superposed folding produced a more or less symmetrical curving of the F_1 axial surfaces. The model was allowed to extend both in the vertical direction and along the strike of the enveloping surface. There was a tightening of the F_2 folds along with a concurrent opening out of F_1. As a result of opening out, there was hinge replacement in certain domains. When the F_1 fold had opened out to a significant extent, superposed buckling was in second mode with small tight F_2 folds riding over larger gentle F_1. With continued deformation, the dip of the enveloping surface increased. When the dip was larger than 45°, both the dip and the strike directions entered in the extension field of the second deformation. As a result, at the late stage of deformation, both F_1 and F_2 started to open out. Both these stages are shown in a single model (Fig. 13) where the enveloping surface is steepened to a great extent in the lower part than in the upper part of the same model.

There were some complex patterns of fold interference when the pitch of the F_1 folds was much less than 90°. In this experiment, the F_1 folds were initially asymmetrical. The asymmetry of the F_1 folds depends upon the angle between the axial surfaces and the enveloping surface. During the second deformation, the sheet-dip of the layer changes and hence the enveloping surface of the F_1 folds was gradually steepened, so that it makes a lower angle with the vertical *X*-axis of strain ellipsoid (Fig. 11b). The generalized axial

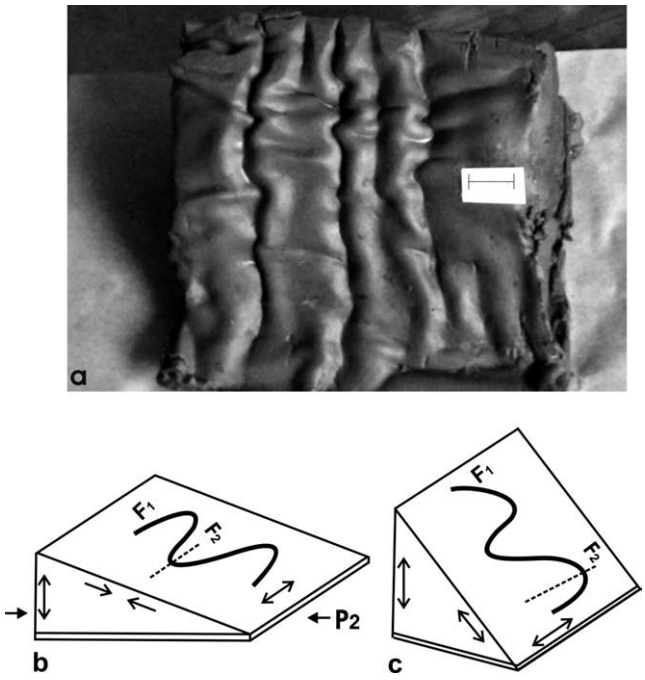

Fig. 13. (a) Superposed buckling of a model with an inclined enveloping surface of early folds. The pitch of F_1 folds is 90°. The layer is curved and is dipping towards the observer. The dip of the enveloping surface is low in the upper part and steep in the lower part. The superposed folds are in modes 2 and 3 in the upper part. Both F_1 and F_2 folds had opened out in the lower part. Scale bar is 1 cm. (b) Schematic sketch of the above model. At the initial stage, the enveloping surface is in the compression field of second deformation. P_2 is the direction of compression during second deformation. (c) With progressive deformation, the enveloping surface has rotated to the extensional field and both F_1 and F_2 folds have opened out.

Fig. 14. Superposed buckling with an inclined enveloping surface. The F_1 folds were horizontal with P_2 parallel to the F_1-axes. The enveloping surface is inclined towards the viewer with a dip of 68°. In the central part, the F_2 and the F_1 folds are subparallel and their interference has produced non-planar sheath folds. Scale bar is 1 cm.

surface of F_1 must also make progressively lower angles with the X-direction. Hence the asymmetry of F_1 folds must increase with progressive deformation during F_2 folding. Within the enveloping surface, the pitch of the generalized direction of F_1 folds also gradually decreases so that it makes a lower angle with the Y-axis. Since the hinge line of F_1 is rotated away from the direction of compression, there must also be a shear parallel to the F_1-axis. Hence the F_2 folds produced by the deformation of F_1 hinge lines and deformation of F_1 folds must also be more and more asymmetric during progressive deformation. The sense of asymmetry can be deduced from the sense of shear as shown in Fig. 11b. Since the bulk deformation is of flattening type, the sheet-dip of the layer will finally increase to such an extent that both F_1 and F_2 folds will open out.

5.4. Superposed buckling of inclined enveloping surfaces with horizontal F_1-axis

In this set of experiments, the F_1 hinge line was horizontal and parallel to the strike of the enveloping surface (Fig. 6d). The dip of the enveloping surfaces varied between 15 and 20°. The F_1 folds were initially asymmetric. The deformation was carried out in pure shear with the shortening direction parallel to the strike of the enveloping surface as well as parallel to the F_1 hinge lines. The model extended only in vertical direction. The relatively tighter segments of F_1 were deformed to a type 2-interference pattern. Since the enveloping surface was extended along the dip, the F_1 folds started to open out and were folded by F_2 in the third mode of superposed buckling, with hinge replacement in certain domains. With progressive deformation, the dip of the layer increased and the layer rotated to the extensional field of second deformation. As a result, the F_2 hinge lines as well as the rotated segments of F_1 hinge lines were both stretched and the angles between two sets of hinge lines were greatly reduced. This caused the development of non-plane non-cylindrical fold in which the rotated F_1 hinge lines on both limbs of F_2 came to lie at a very low angle with the F_2-axis. In the final stage, F_1- and F_2-axes became subparallel and the resulting folds were non-planar sheath folds (Fig. 14).

Non-planar sheath folds (Ghosh et al., 1999) are

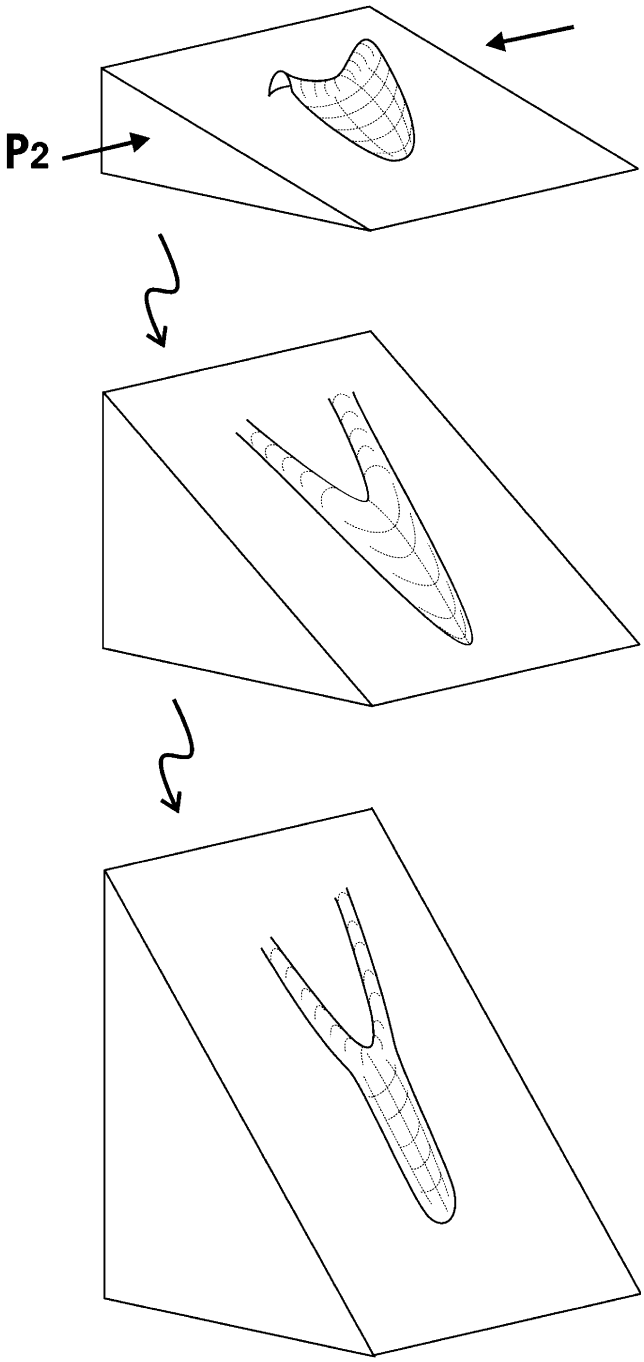

Fig. 15. Simplified sketch showing successive stages of formation of non-planar sheath fold from an early cylindrical fold during second deformation.

sheath-like structures but with strongly curved axial surfaces and with subparallel orientation of F_1 and F_2 hinge lines in the major part of the structure. Morphologically, it resembles folded sheath folds. However, unlike refolded sheath folds, the sheath-like geometry is produced during folding of early cylindrical folds. Fig. 15 shows a schematic diagram illustrating the progressive stages of formation of a non-planar sheath fold from an early cylindrical fold during the second deformation.

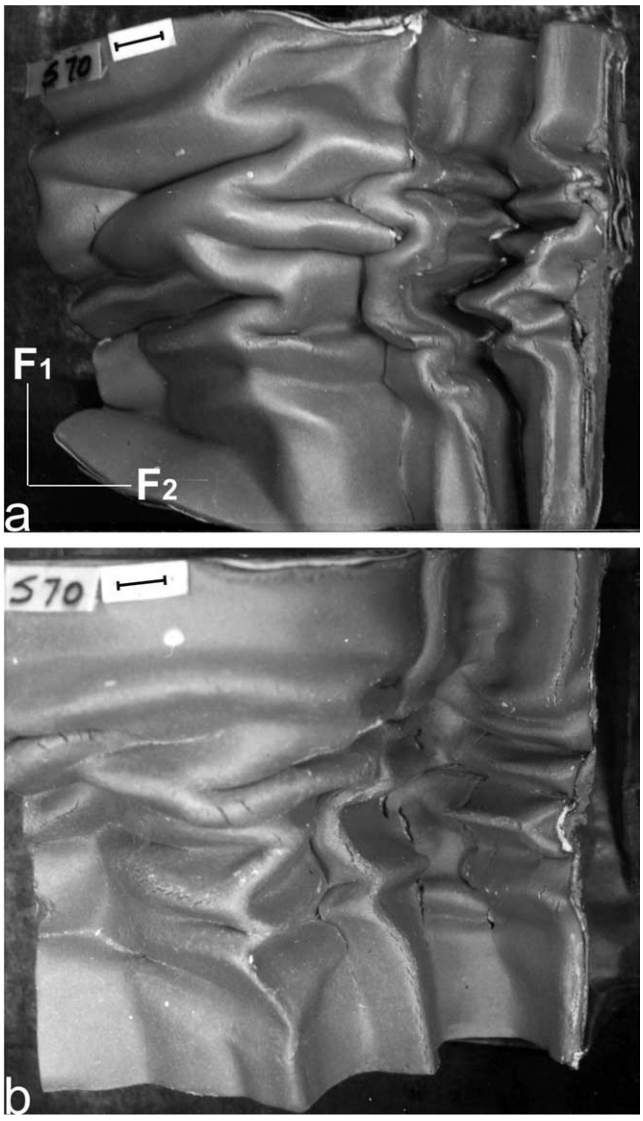

Fig. 16. Deformation of early chevron folds in multilayer. (a) and (b) show fold interference at two levels after removal of the overburden at different levels. Scale bar is 1 cm.

5.5. Opening out of chevron folds in multilayers with P_2 parallel to F_1-axes

These experiments showed that the process of hinge replacement and the development of the third mode of superposed buckling are largely inhibited when F_1 is a chevron fold. In the model shown in Fig. 16a, sharp-hinged F_1 folds at one level of the multilayer were deformed to sharp-hinged F_2 folds in a type 2 interference pattern in the fourth mode of superposed buckling without any hinge replacement. On the left side, however, the F_1 folds were more open and had moderate sharpness of hinges, and superposed buckling was by the third mode with some hinge replacement. Fig. 16b shows the same model at a still lower level where the F_1 folds were sharp-hinged in most places.

Superposed buckling was mostly by fourth mode without any hinge replacement.

6. Natural examples of opening out of early folds

The interpretation of the field structures is based on the conclusion that a type 1 interference pattern of buckling folds cannot develop if F_1 is tight or isoclinal. This conclusion is supported by all previous experiments (Ghosh and Ramberg, 1968; Skjernaa, 1975; Watkinson, 1981; Ghosh et al. 1992, 1993, 1996; Grujic 1993). In most natural examples of superposed folds, the earliest fold is generally described as the tightest. Successive later folds are described as more and more open. There is, however, no reason why the earliest shortening will always be the largest. During development of type 2 interference pattern, rotated F_1 folds of moderate tightness may become very tight or isoclinal during the second deformation. In some cases, at least, the F_1 folds may open out during the second deformation.

In the neighborhood of Singhbhum shear zone in eastern India (Ghosh and Sengupta, 1987), the reclined F_1 folds are generally very tight or isoclinal and F_1/F_2 interference has produced a type 2 interference. There is a strongly developed intersection lineation as well as a stretching lineation parallel to the F_1-axis. In certain domains, however, F_1 is very gentle and F_1/F_2 interference produced a dome-and-basin pattern. Here we see F_2 folds and much gentler F_1 folds parallel to the F_1 intersection and stretching lineation. The tight F_1 folds are absent (Fig. 17a). Superposition of F_2 folds on very gentle F_1 in a type 1 interference pattern can be best explained by assuming that F_1 has opened out in these domains.

A similar feature can also be seen in certain parts of Aravalli metasediments near Udaipur, in Rajasthan, western India (Fig. 17b). Here too F_1 is tight or isoclinal in most parts. A strong stretching lineation is parallel to the F_1-axis. However, in certain domains, the F_1 folds parallel to the L_1 stretching lineation are very gentle. L_1 is deformed by nearly isoclinal F_2 folds. The structure, very similar to the experimental structure shown in Fig. 10, suggests that during the development of F_2, F_1 had opened out to a large extent.

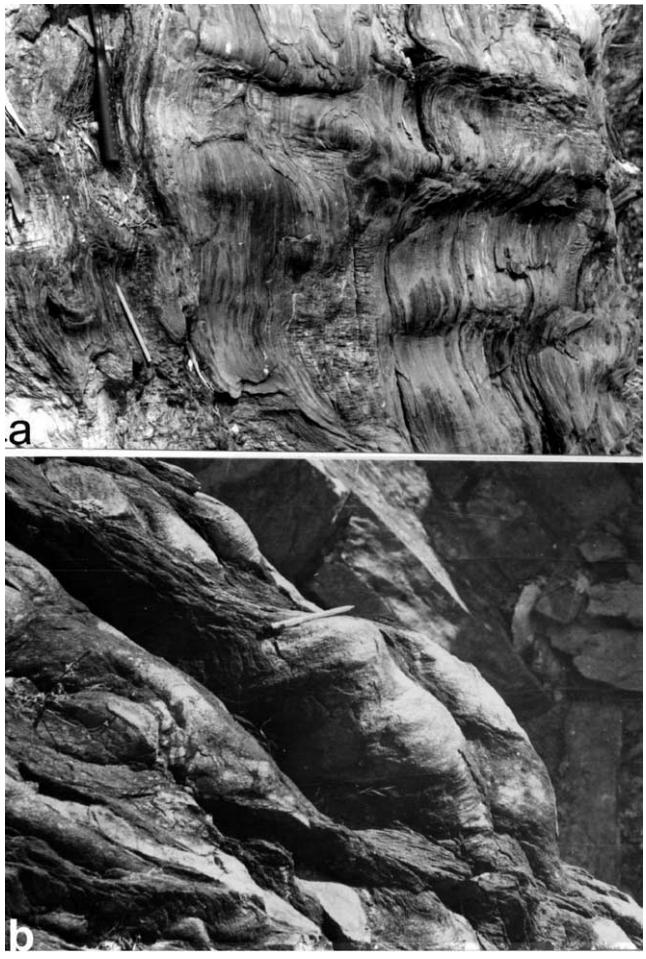

Fig. 17. (a) Interference of two sets of folds in Singhbhum, eastern India. The early folds parallel to the lineation (and hammer) are open and produced a dome-and-basin pattern with F_2. (b) Opening out of F_1 (parallel to the lineation) folds in Aravalli metasediments, Udaipur, Rajasthan. Pencil parallel to F_1. F_2 folds are very tight or isoclinal. The structure is very similar to the model shown in Fig. 10b.

7. Discussion

The numerical calculations from the theoretical model are in agreement with the experimental results of opening out of folds during superposed deformation. Thus, at any constant rate of extension across the axial surface of F_1, the rate of opening out (i.e. the rate of increase of the interlimb angle with respect to bulk extensional strain rate) is very sensitive to the initial tightness. A tight fold opens out at a much smaller rate than a less tight fold. Hence if we have a small range of initial tightness of F_1 in a domain, the range of tightness may greatly increase during superposed deformation involving the opening out of early folds. The opening out is dependent to a much smaller extent on the ratio of rates of external rotation and homogeneous strain. If this ratio is small, there is a significant increase in the length of arc of the folds provided the initial fold was not very tight. For all folds, the rate of opening out increases with progressive deformation. Consequently, a nearly isoclinal or very tight fold remains tight even to a moderately large bulk extension across its axial plane. Moderately tight or close folds may open out to a great extent at a relatively small value of deformations.

This conclusion from the numerical model is supported by the experiments. Thus, if F_1 is isoclinal, superposed buckling may not be in the fourth mode when the deformation involves an opening out. The resulting F_2 is mostly in modes 3 or 2. Again, if F_1 initially has a moderate tightness, we may have an unusual situation in which small

tight F_2 folds ride over very gentle F_1. These experiments showed that the early folds might not always be the tightest. The extent of opening out depends to a great extent on the initial tightness. Since the initial tightness of F_1 generally varies from domain to domain, a wide range of opening out and a wide range of morphology of superposed folds are expected to occur when an opening out of F_1 is involved. The inhomogeneous nature of opening out may give rise to a variety of superposed structures. In certain situations, the superposed folds may give rise to non-planar sheath folds.

The experiments also suggest that the final geometry of the fold interference is controlled by a delicate balance between the rate of opening out of F_1 and the rate of buckle shortening across F_1 axial surface. If the rate of buckle shortening relative to the rate of opening out is very large, the mode of superposed buckling is controlled by the initial tightness of F_1. Subsequent extension across F_1 axial surface modifies the geometry of both F_1 and F_2 but does not change the buckling mode produced at an early stage. On the other hand, if the ratio of rate of buckle shortening to rate of opening out is not so large, the mode of superposed buckling does not provide us a clue to the initial tightness of F_1 folds. The buckling mode will depend on the extent of opening out of F_1 before the initiation of F_2 folds. Depending on the amount of initial phase of opening out of F_1, refolding of tight or isoclinal early folds may take place in any of the four modes. Once a particular mode of superposed buckling is produced, the F_1 folds may continue to open out while F_2 is progressively tightened. Since relative rates of buckle shortening may vary in distinct domains, we may get a close association of different modes.

Transformation of a plane cylindrical fold into a non-plane non-cylindrical fold by superposed deformation presents an important kinematic problem. The bending of the axial surface and the hinge line of a competent layer involves shear strain along the curved hinge line. Ramsay (1967, p. 547) has indicated that such a large hinge-parallel shear could cause a slide or fault along the hinge line. Since such features along the curved hinge lines of superposed folds are not generally found, there must be some other process associated with development of a type 2 interference pattern by deformation of cylindrical non-isoclinal buckling folds. The process, which has been described in our earlier papers as 'hinge replacement' (Ghosh et al., 1992, 1996), associated with the development of non-planar non-cylindrical fold from a plane cylindrical fold, is distinct from the process of hinge migration (Odonne and Vialon, 1987) which may not involve the development of type 2 interference pattern.

Consider a non-isoclinal plane cylindrical F_1 fold with the material line H along its hinge (Fig. 18a). If the initial fold is tight with a very small interlimb angle, a type 2 interference is produced in the fourth mode of superposed buckling. The limbs A and B after superposed deformation intersect along the curved line H (Fig. 18b). If, on the other hand, the superposed deformation involves an opening out

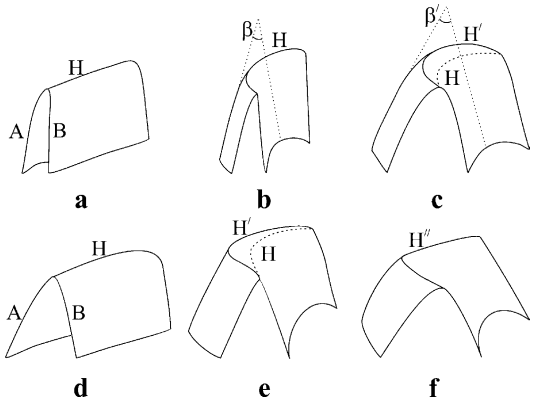

Fig. 18. Hinge replacement in superposed buckling with or without opening out. (a) Initial fold very tight with limbs A and B. (b) Superposed fold in mode 4 without hinge replacement. The angle between the two F_2 folds on A and B is β. (c) If there is an opening out, the angle β increases to β', A and B can no longer intersect along H; they then intersect along a strongly curved hinge line H'. (d) Initial fold moderately tight. (e) Superposed folding in mode 3 with F_2 folds on A and B intersecting along a curved line H' which is produced by replacing the material line H. (f) If there is an opening out, the angle β increases to β' and a new hinge line H'' is produced by hinge replacement.

of the F_1 fold, the angle β (Fig. 18b and c) increases. The folds on A and B can no longer intersect along H. They then intersect along the line H' (Fig. 18c) which is quite different from the material line H. If the initial fold was not so tight (Fig. 18d), the deformation of F_1 may produce a type 2 interference in the third mode with hinge replacement (Fig. 18e). If there is an opening out of the F_1, with increase in the angle β (Fig. 18f), the geometrical transformation can only be by hinge replacement. The process of hinge replacement takes place because it consumes less strain. Since the opening out of an F_1 fold involves an increase in the angle of β (Fig. 18), the process of opening out of F_1 in a type 2 interference pattern invariably involves hinge replacement.

Acknowledgements

We wish to thank the Council of Scientific and Industrial Research, India, for financial support. We are grateful to Peter Hudleston, Francis Odonne and Djordje Grujic for critical comments and helpful suggestions.

References

Belyakov, V.M., Kavtsova, P.I., Rappopart, M.G., 1965. Tables of Elliptic Integrals. Part I. Pergamon Press, Oxford.

Flinn, D., 1962. On folding during three-dimensional progressive deformation. Quaternary Journal of Geological Society of London 118, 385–433.

Ghosh, S.K., Chatterjee, A., 1985. Patterns of deformed early lineations over later folds formed by buckling and flattening. Journal of Structural Geology 7, 651–666.

Ghosh, S.K., Ramberg, H., 1968. Buckling experiments on intersecting fold patterns. Tectonophysics 5, 89–105.

Ghosh, S.K., Sengupta, S., 1987. Progressive development of structures in a ductile shear zone. Journal of Structural Geology 9, 277–287.

Ghosh, S.K., Mandal, N., Khan, D., Deb, S.K., 1992. Modes of superposed folding in single layers controlled by initial tightness of early folds. Journal of Structural Geology 14, 381–394.

Ghosh, S.K., Mandal, N., Sengupta, S., Deb, S.K., Khan, D., 1993. Superposed buckling in multilayers. Journal of Structural Geology 15, 95–111.

Ghosh, S.K., Khan, D., Sengupta, S., 1995. Interfering folds in constrictional deformation. Journal of Structural Geology 17, 1361–1371.

Ghosh, S.K., Deb, S., Sengupta, S., 1996. Hinge migration and hinge replacement. Tectonophysics 263, 319–337.

Ghosh, S.K., Hazra, S., Sengupta, S., 1999. Planar, nonplanar and refolded sheath folds in the Phulad Shear zone, Rajasthan, India. Journal of Structural Geology 21, 1715–1720.

Grujic, D., 1993. The influence of initial fold geometry on Type 1 and Type 2 interference pattern: an experimental approach. Journal of Structural Geology 15, 293–307.

Grujic, D., Walter, T.R., Gártner, H., 2002. Shape and structure of analogue models of refolded layers. Journal of Structural Geology 24, 1313–1326.

Hancock, H., 1958. Elliptic Integrals. Dover, New York.

Johns, M.K., Mosher, S., 1996. Physical models of regional fold superposition: the role of competence contrast. Journal of Structural Geology 18, 475–492.

Odonne, F., Vialon, P., 1987. Hinge migration as a mechanism of superposed folding. Journal of Structural Geology 9, 835–844.

Ramsay, J.G., 1962. Interference pattern produced by the superposition of folds of "similar" type. Journal of Geology 60, 466–481.

Ramsay, J.G., 1967. Folding and Fracturing of rocks. McGraw-Hill, New York.

Ramsay, J.G., Huber, M.I., 1987. The Techniques of Modern Structural Geology, Folds and Fractures, vol. 2. Academic Press, London.

Skjernaa, L., 1975. Experiments on superimposed buckle folding. Tectonophysics 27, 255–270.

Watkinson, A.J., 1981. Patterns of fold interference: influence of early fold shapes. Journal of structural Geology 3, 19–23.